Measurement of ω-Meson Photoproduction on Protons from 46 to 180 GeV

R. M. Egloff, P. J. Davis, G. J. Luste, J.F. Martin, and J. D. Prentice
University of Toronto, Toronto, Ontario M5S 1A7, Canada

and

D. O. Caldwell, J. P. Cumalat,[a] A. M. Eisner, A. Lu, R. J. Morrison, and S. J. Yellin
University of California, Santa Barbara, California 93106

and

T. Nash
Fermi National Accelerator Laboratory, Batavia, Illinois 60510
(Received 24 September 1979)

Elastic ω-meson photoproduction on protons has been measured from 46 to 180 GeV. The cross section is approximately constant with photon energy and averages 1.10 $\pm$ 0.08 μb. The t dependence of the differential cross section is consistent with $A\exp(bt)$, where $b = 8.4 \pm 0.7$ GeV^{-2}. The photon-omega coupling constant, obtained from a normalization of hadron elastic-scattering cross sections to the photoproduction data of this experiment (with use of vector-meson dominance and an additive quark model), is $\gamma_\omega^2/4\pi = 5.4 \pm 0.4$.

Elastic ω photoproduction on protons has been measured from 46 to 180 GeV at the Tagged-Photon Laboratory of Fermilab. ρ and φ photoproduction cross sections have been published previously.[1] The data were taken during photon total cross-section measurements.[2,3]

The ω was detected by its all-neutral decay, $\omega \to \pi^0\gamma \to \gamma\gamma\gamma$ (branching ratio = 8.8%), with all three photons measured in two lead-glass shower-counter arrays. The Pb-glass arrays, G2 and G3, are shown schematically in Fig. 1. The C counter was a lead-scintillator shower counter located in the beam region downstream of G3. Four scintillation recoil detectors surrounded a 1-m-long liquid hydrogen target. Other detectors (not shown in the figure for clarity) consisted of six multiwire proportional chambers (MWPC's), located in front of G3, and several multilayer lead-iron scintillator counters. More details on the detection apparatus can be found in Ref. 2. The apparatus was moved along the beam direction to scale the acceptance geometry for different electron beam energies, E_0. Data were taken with $E_0 = 90$, 135, and 200 GeV, resulting in tagged-photon energy from 46 to 180 GeV.

An event was considered an elastic $\omega \to \pi^0\gamma$ candidate if it had three photons of energy greater than 1 GeV incident on G2 and G3. The electromagnetic energy in G2, G3, and C was required to be at least 90% of the tagged incident-photon energy. The 10% error margin allowed for the energy resolution of the apparatus and beam, and shower leakage for photons incident near the inside edges of the Pb-glass counters surrounding the central hole in G3 and, more importantly, G2. The lead-iron scintillator counters in the apparatus were used to veto events which were inconsistent with exclusive three-photon final states.

Events with more than one track in the MWPC's were rejected. If there was one track, its position given by the MWPC's had to agree with a shower position in G3. Most accepted events have zero chamber tracks. There is, however, a 10% to 20% probability (acceptance dependent) for one track due to a $\gamma \to e^+e^-$ conversion in the hydrogen target or the vacuum window just upstream of the MWPC's.

The two-photon invariant-mass spectrum for events surviving the analysis cuts for $\omega \to \pi^0\gamma$ candidates is shown in Fig. 2(a). Each event contributes three two-photon combinations. About $\frac{1}{3}$ of the conbinations peak in the π^0 mass region, indicating that most events are compatible with a $\pi^0\gamma$ state. The π^0 candidate for each event was

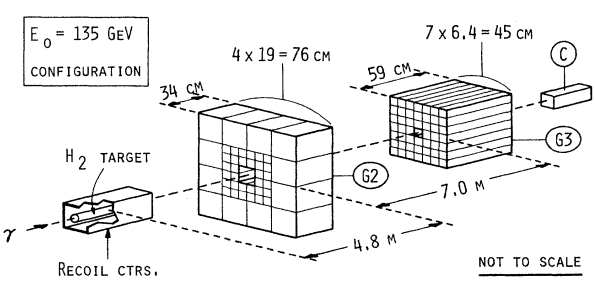

FIG. 1. Simplified schematic of apparatus, showing lead-glass shower-counter arrays G2 and G3.

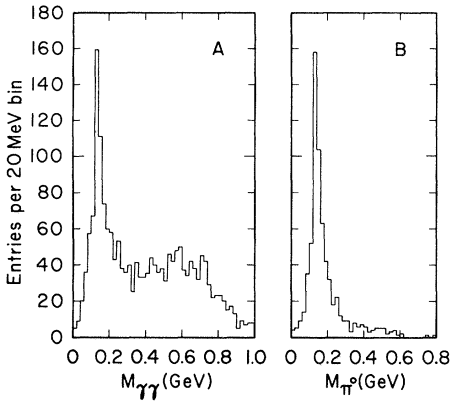

FIG. 2. Two-photon invariant-mass spectrum for $\omega \to \pi^0\gamma$ candidates. Each event gives three $M_{\gamma\gamma}$ combinations, shown in (a). In (b) only the combination nearest the π^0 mass (one per event) is shown.

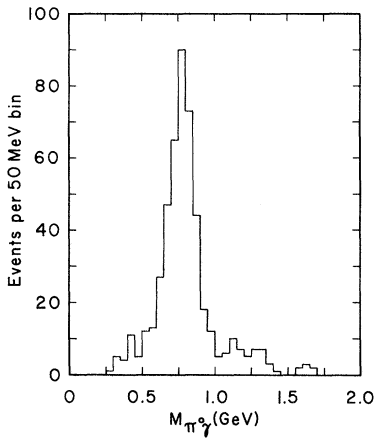

FIG. 3. Three-photon invariant-mass spectrum for events passing all analysis cuts.

chosen to be that photon pair with a mass nearest to 135 MeV. The resulting two-photon mass distribution is shown in Fig. 2(b).

The three-photon invariant-mass spectrum for events which have a two-photon combination between 80 and 220 MeV is shown in Fig. 3. The mass distribution shows a clear peak at the ω mass (783 MeV). The width of the peak is dominated by the energy and position resolution of the photon-shower reconstruction and by the uncertainty of the ω-decay vertex position, assumed to be at the center of the hydrogen target. The energy and position distributions of the photons in G3 and G2 agree well with Monte Carlo–generated distributions for $\omega \to \pi^0\gamma$ production.

The decay polar angle distribution in the helicity frame for $\omega \to \pi^0\gamma$ (J^P: $1^- \to 0^- + 1^-$) is shown in Fig. 4. The number of events in each $\cos\theta$ bin is corrected for acceptance losses. The angular dependence expected for s-channel helicity conservation (SCHC) is $1 + \cos^2\theta$, shown by the curve in Fig. 4. The data are consistent with SCHC, in agreement with lower-energy measurements.[4]

For the calculation of the ω photoproduction cross section, the observed yield of $\pi^0\gamma$ events above background was corrected for events lost because of the geometric acceptance of the apparatus, the event reconstruction efficiency, and the analysis cuts used to select $\omega \to \pi^0\gamma$ candidates. The correction factor, as determined by a Monte Carlo simulation of the entire analysis procedure, averages 3.04. The number of background events was obtained from a fit of the mass distribution at each of the three electron beam energies. It ranges from 10% to 20% of the events in the ω mass region. The correction factor for the contribution of $\rho \to \pi^0\gamma$ events is 0.98.[5]

The cross section is also corrected for inelastic ω photoproduction, $\gamma p \to \omega X$, where X represents a target dissociation (or excitation) with no detected downstream products. Elastic and inelastic events can be statistically distinguished by their different probabilities for firing $n = 0$, 1, or > 1 or the four recoil counters surrounding the hydrogen target. Elastic events are expected to have $n = 0$ or $n = 1$ (usually $n = 0$), with probabilities computable from range-energy relations. Inelastic events almost always have $n = 1$ or $n > 1$ (usually $n > 1$), with probabilities determined from a simple Poisson model which agrees with hadronic studies of target dissociation.[6] Our results are not very sensitive to details of the model. The inelastic-event contribution was determined to be $(26 \pm 4)\%$.[7]

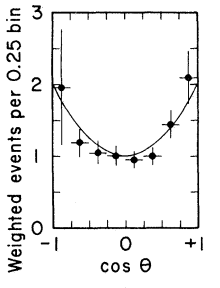

FIG. 4. Decay polar-angle distribution in the helicity frame for $\omega \to \pi^0\gamma$. The curve has the form $1 + \cos^2\theta$.

TABLE I. The elastic cross section, $\sigma(\gamma p \to \omega p)$, with statistical uncertainties.

E_0 (GeV)	E_γ (GeV)	σ (μb)
90	53 ± 7	1.17 ± 0.18
90	71 ± 11	1.04 ± 0.16
135	95 ± 27	1.11 ± 0.13
200	140 ± 40	1.08 ± 0.18

Another criterion for elastic ω production is the coplanarity of the recoil proton and the ω. The direction (specifically, the azimuthal angle) of the recoil proton can be predicted from the ω direction of flight calculated from the measured energies and positions of the decay photons. An event with a recoil signal in a counter other than the one predicted from the calculated recoil proton direction may be classified as inelastic. The fraction of inelastic events thus determined agrees with the inelastic-event contribution obtained with use of the statistical method.

The elastic ω photoproduction cross section is given in Table I and shown in Fig. 5 with some lower-energy data.[8] The quoted errors are statistical and include the uncertainty due to the correction for inelastic events. The systematic uncertainty was estimated to be ± 8% for all data points and is primarily due to the geometric acceptance, including the shower reconstruction efficiency.

The differential cross section for ω photoproduction was determined from a fit to the data of the form

$$d\sigma/dt = Ae^{-b|t|}, \quad (1)$$

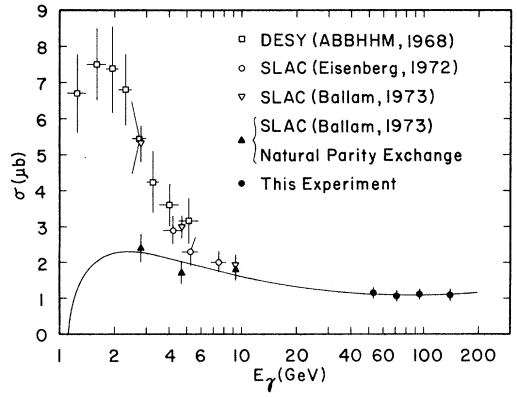

FIG. 5. Energy dependence of the ω photoproduction cross section. The curve is a VMD–quark-model prediction normalized to the data of this experiment.

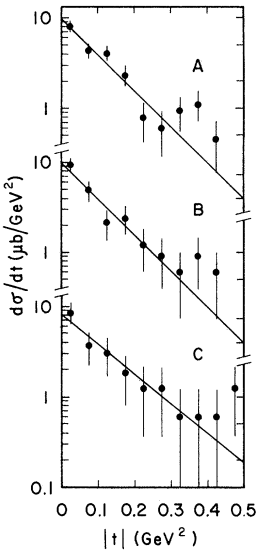

FIG. 6. Differential cross section for elastic ω photoproduction A, B, and C correspond to electron beam energies E_0 = 90, 135, and 200 GeV. The lines are fits of the form $d\sigma/dt = A \exp(bt)$.

where t is the four-momentum transfer squared. Events with greater than one recoil counter signal, or a recoil signal in a counter which is inconsistent with the predicted recoil proton direction (azimuthal angle) calculated from the ω direction of flight, were not included in the fit. This eliminated most inelastic events which are expected to have a smaller value of b than elastic events. The t distributions are shown in Fig. 6. The fitted parameters A and b are given in Table II. The values of b are consistent with those measured for ρ and ω photoproduction at lower energies and with the average slope of $\pi^+ p$ and $\pi^- p$ elastic scattering.

In vector-meson–dominance (VMD) models, photoproduction of the ω is related to ωp elastic scattering. The ωp scattering can in turn be related to πp elastic scattering by additive-quark-model relations. The photoproduction cross sec-

TABLE II. The forward differential cross section and slope from a fit to the elastic data of the form $d\sigma/dt\,(\gamma p \to \omega p) = A \exp(bt)$.

E_0 (GeV)	E_γ (GeV)	A (μb/GeV^2)	b (GeV^{-2})
90	64 ± 18	9.90 ± 1.33	9.05 ± 1.00
135	95 ± 27	10.11 ± 2.11	9.11 ± 1.66
200	140 ± 40	8.10 ± 2.51	7.52 ± 2.14
Combined data		9.24 ± 0.96	8.42 ± 0.74

tion is then given by

$$\sigma(\gamma p \to \omega p) = \frac{p_\pi^2}{k_\gamma} \frac{e^2}{4\gamma_\omega^2} \frac{1}{2} [\sigma^{el}(\pi^+ p) + \sigma^{el}(\pi^- p)] \times \exp(-b|t_{min}|), \quad (2)$$

where p_π and k_γ are the momenta of the π and the photon, respectively, in the πp and γp center-of-mass systems (evaluated at the same s). Here γ_ω^2 is the γ-ω coupling constant, and the factor $\exp(-b|t_{min}|)$ allows for the minimum $|t|$ in ω photoproduction. Equation (2) is plotted in Fig. 4 with use of smoothed πp elastic-scattering data.[9] The curve is normalized to the ω cross section of this experiment. The value of the coupling constant resulting from the normalization is

$$\gamma_\omega^2/4\pi = 5.4 \pm 0.4,$$

and compares with 4.6 ± 0.5 from colliding-beam measurements[10] and 7.5 ± 1.3 from photoproduction on complex nuclei.[10] The deviation of the lower-energy ω cross section from the VMD–quark-model prediction is attributed to unnatural-parity (pion) exchange in the t channel, which decreases with increasing photon energy approximately as $1/E^2$. The cross section which is due to natural-parity exchange only has been measured by Ballam *et al.*[4] and is also shown in Fig. 4. There is good agreement with the VMD–quark-model prediction.

We gratefully acknowledge support from the staffs of Fermilab, the University of Toronto, and the University of California at Santa Barbara. Valuable assistance was provided by F. Murphy, M. Franklin, and M. G. Donnelly and also by A. Belousov and B. Govorkov of the Lebedev Physical Institute. This research was supported in part by the U. S. Department of Energy and by the National Research Council of Canada through the Institute of Particle Physics of Canada.

[a]Present address: Fermi National Accelerator Laboratory, Batavia, Ill. 60510.

[1]R. M. Egloff *et al.*, Phys. Rev. Lett. 43, 657 (1979).

[2]D. O. Caldwell *et al.*, Phys. Rev. Lett. 40, 1222 (1978); J. P. Cumalat, thesis, University of California, Santa Barbara, 1977 (unpublished).

[3]D. O. Caldwell *et al.*, Phys. Rev. Lett. 42, 553 (1979).

[4]J. Ballam *et al.*, Phys. Rev. D 7, 3150 (1973).

[5]$\sigma(\gamma p \to \rho p) = 9.3$ μb from Ref. 1, and $\rho \to \pi^0\gamma$ branching ratio = 0.024%.

[6]J. Whitmore, Phys. Rep. 10C, 273 (1974).

[7]This fraction is consistent with diffraction-dissociation cross sections measured in pp and πp scattering: See Ref. 6 and also M. G. Albrow *et al.*, Nucl. Phys. B108, 1 (1976); G. Wolf, Nucl. Phys. B26, 317 (1971).

[8]Aachen-Berlin-Bonn-Hamburg-Heidelberg-Munchen Collaboration, Phys. Rev. 175, 1669 (1968); Y. Eisenberg *et al.*, Phys. Rev. D 5, 15 (1972); J. Ballam *et al.*, Phys. Rev. D 7, 3150 (1973).

[9]D. S. Ayres *et al.*, Phys. Rev. D 15, 3105 (1977); K. J. Foley *et al.*, Phys. Rev. Lett. 11, 425 (1963); I. Ambats *et al.*, Phys. Rev. D 9, 1179 (1974).

[10]D. W. G. S. Leith, in *Electromagnetic Interactions of Hadrons*, edited by A. Donnachie and G. Shaw (Plenum, New York, 1978).

Calculability in $SU(2)_L \otimes SU(2)_R \otimes U(1)$: The Mass Matrix and *CP*-Invariance Violation

Arthur C. Rothman and Kyungsik Kang
Physics Department, Brown University, Providence, Rhode Island 02912

(Received 27 July 1979)

It is shown that calculability of the mixing angles in a class of n-generation, left-right-symmetric $SU(2)_L \otimes SU(2)_R \otimes U(1)$ models restricts the fermion mass matrix to be of the form $\Sigma_{m=0}^{n} \oplus I_m A_m$ with the constraint $\Sigma_{m=0}^{n} m I_m = n$, where A_m is a nonsingular $m \times m$ Hermitian or complex symmetric block containing $2m-1$ elements and I_m is the number of such blocks. Such a mass matrix *cannot* supply *CP*-invariance-violating phases.

There have been, in the last few years, many attempts to derive expressions for the Cabibbo mixing angles, θ_i, as a function of quark masses only. These results were obtained by requiring the Lagrangian to be invariant under additional symmetries—Abelian[1] or non-Abelian[2] discrete models only slightly distort the initial spectrum tries—above and beyond the specific gauge group employed. The motivation for these works has been "calculability." Flavor mixing from the standpoint of natural flavor conservation is discussed elsewhere.[4] In some of these models[5] a mechanism combining the *CP*-invariance-violating phases and mixing angles was generated by